MINERALOGY OF OLIVINE XENOCRYSTS IN ASUKA 12209 ANGRITE. T. Mikouchi[1], A. Yamaguchi[2], V. Debaille[3], S. McKibbin[4], S. Goderis[4], L. Pittarello[5], N. Shirai[6], G. Hublet[2], G. Quitté[7], T. Iizuka[1], R. C. Greenwood[8], P. Claeys[4], [1]The University of Tokyo, Tokyo, Japan, [2]National Institute of Polar Research (NIPR), Tokyo, Japan, [3]Université Libre de Bruxelles, Brussels, Belgium, [4]Vrije Universiteit Brussel, Brussels, Belgium, [5]University of Vienna, Vienna, Austria, [6]Tokyo Metropolitan University, Tokyo, Japan, [7]IRAP, Observatoire Midi-Pyrénées, Toulouse, France, [8]Open University, Milton Keynes, UK, E-mail: mikouchi@eps.s.u-tokyo.ac.jp.

Introduction: Asuka 12209 (A 12209) is a "quenched" angrite that was collected by the joint Japanese and Belgian Antarctic meteorite research expedition (JARE54 and BELARE-SAMBA) during the 2012-2013 season [1,2]. It is a 43.65 g complete stone only partly covered with fusion crust. The surface color is dark brown with xenocrystic olivine megacrysts (up to 5 mm) exposed on the fine-grained surface. Our earlier study showed that it was likely to be paired with Asuka-881371 (A-881371) based on their almost identical petrology and mineralogy [3,4]. Because A-881371 is only 11.3 g, the finding of this larger sample will allow us analyses using more sophisticated instruments. We are undertaking a consortium study of A 12209 from the viewpoint of its mineralogy, geochemistry and physical properties. In this abstract we discuss the ongoing mineralogical studies of olivine xenocrysts in A 12209, which are aimed at understanding their origin and mode of incorporation into the angrite groundmass magma. These results are combined with those from other xenocrystic olivine-bearing quenched angrites, such as Lewis Cliff 87051 (LEW 87051) and Northwest Africa 1670 (NWA 1670).

Sample and Methods: A polished thin section (PTS) of A 12209 was first studied by optical microscopy to carefully observe any deformation features present in the olivine xenocrysts. Then, mineral compositions were determined by electron microprobe (JEOL JXA-8530F) at the University of Tokyo after the X-ray elemental maps were obtained. Analytical conditions of 25 kV accelerating voltage and 50 nA beam current with 50 sec counting time at peaks were employed to accurately analyze minor elements in olivine. We also used a FEG-SEM-EBSD system at NIPR (JEOL JSM-7100F/Oxford AZtek) for EBSD analysis of olivine xenocrysts.

Results: The PTS studied shows a fine-grained ophitic texture with large olivine xenocrysts up to 4 mm in diameter. The X-ray elemental mapping revealed 17 xenocrystic olivine grains in the PTS studied that can be distinguished from phenocrystic olivine by their distinct Mg-rich compositions (Fig. 1). All large olivine grains exceeding 1 mm have homogeneous Mg-rich compositions except for ~100 μm overgrown rims co-crystallized with olivine phenocrysts. The olivine compositions of the xenocrysts (core composition) are Fo_{90-83}, which are overlapping with those in A-881371 [5]. Phenocrystic olivines have Fo_{75} core and are zoned to extremely Fe-Ca-rich compositions at complex fayalite-kirschsteinite intergrowth. Some of the xenocrysts are present only as the small cores to later overgrown olivine phenocrysts (Fig. 1). All xenocrystic olivines have more Cr-rich (Cr_2O_3=0.20-0.45 wt%) and Ca-poor (CaO=0.15-0.45 wt%) compositions compared to phenocrysts (<0.1 wt% Cr_2O_3 and >0.6 wt% CaO). Tiny Fe-Ni metal and sulfides are present in olivine xenocrysts, and they are sometimes aligned along fractures. This observation is also similar to A-881371 [6].

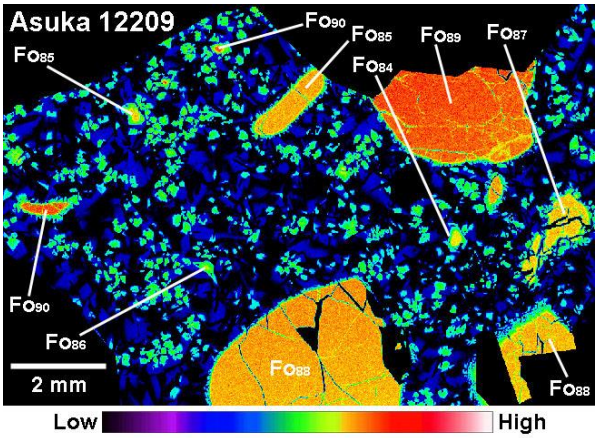

Fig. 1. Mg X-ray map of A 12209. Note the presence of large olivine grains with different olivine compositions (red~orange). Green color is phenocrystic olivine.

A remarkable characteristic of olivine xenocrysts in A 12209 is their variable degrees of deformation features although the fine-grained groundmass shows no evidence for deformation. Some xenocryst grains show sharp extinction under optical microscope, but kink bands are common for many other grains. A few grains show tilt boundaries and partial recrystallization is found in such grains (Fig. 2). This observation is mostly consistent with olivine xenocrysts in A-881371 [6,7], but A 12209 contains xenocrysts showing more pronounced tilt boundaries. This is probably because of the larger size of the A 12209 PTS compared to that of A-881371 and thus A 12209 contains more xenocryst grains. There is no correlation between degrees of de-

formation and olivine composition, as also observed for A-881371 [7].

We expected to see variable band contrast values of Kikuchi bands obtained by EBSD analysis for olivine xenocrysts due to different degrees of deformation as observed by optical microscopy, but the difference was not clear. The tilt boundaries and recrystallized portions of olivine xenocrysts clearly show different orientations by EBSD (Fig. 2).

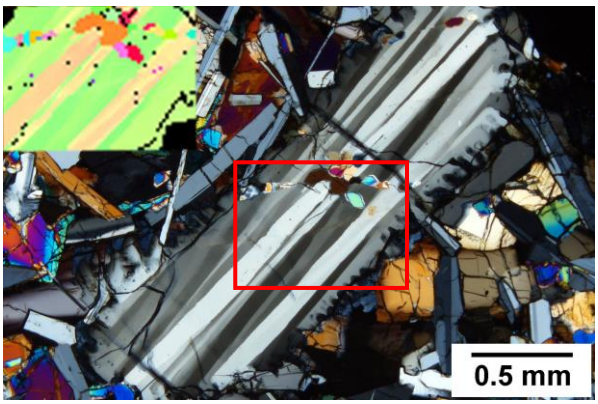

Fig. 2. Cross polarized photomicrograph of olivine xenocryst showing tilt boundaries and partial recrystallization. The image at the upper left corner is an orientation map by EBSD (red rectangle in the optical image), reflecting different orientations of olivine grains.

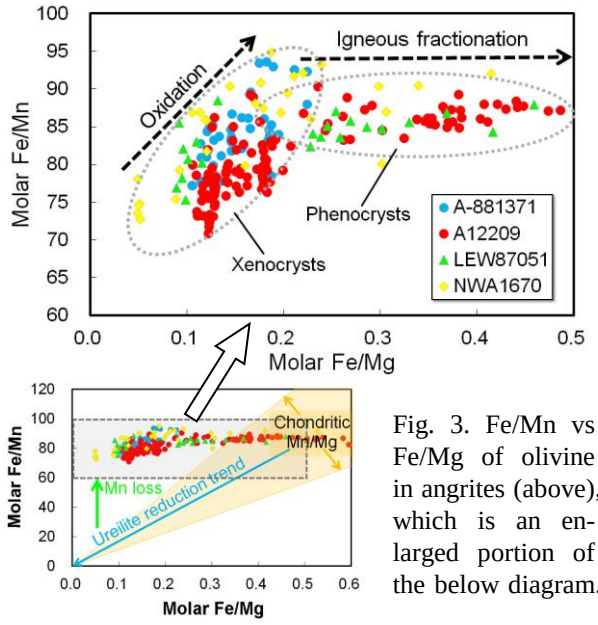

Fig. 3. Fe/Mn vs Fe/Mg of olivine in angrites (above), which is an enlarged portion of the below diagram.

We plotted molar Fe-Mg-Mn contents of both xenocrystic and phenocrystic olivine in A 12209 and A-881371 with those in LEW 87051 and NWA 1670 in the Fe/Mg vs Fe/Mn diagram that is often used for ureilites and primitive achondrites [e.g., 8] (Fig. 3). We found that olivine xenocrysts in Asuka angrites show a positive trend while phenocrysts are only variable on Fe/Mg with constant Fe/Mn, corresponding to normal igneous fractionation.

Discussion and Conclusion: Deformation features in olivine xenocrysts are more pronounced in A 12209 than A-881371, and our study demonstrates that olivine xenocrysts in Asuka angrites experienced variable degrees of deformation prior to incorporation within the groundmass melt. So the question is how and when this took place. As was discussed in [7], one idea is that they formed by shock metamorphism, suggesting that quenched angrites are impact melt rocks. A similar petrogenesis for the quenched angrites was proposed by [9]. An alternative proposal is that the olivine xenocrysts are derived from the mantle of the angrite parent body and that deformation reflects mantle rheology [6,7]. However, it is unclear which hypothesis is more likely. Probably, more detailed EBSD analysis of recrystallized olivine will help to clarify their origin.

A novel finding from this new angrite is that Fe/Mn and Fe/Mg of olivine xenocrysts show a redox variation rather than igneous fractionation (Fig. 3). Olivine xenocrysts in LEW 87051 and NWA 1670 are found to have similar trends. Because the plots are offset from the normal redox trend found for ureilites and chondritic values towards Mn-poor compositions, it is likely that Mn was lost before olivine crystallized. Since Mn is a moderately volatile element, Mn might be lost by volatilization from the xenocryst precursor. This is consistent with extremely low alkali contents of angrites. The phenocrystic olivine has Fe/Mn of 85-90. This means that the redox trend found for olivine xenocrysts can be interpreted to result from oxidation of Mg-rich olivine that originally had lower Fe/Mn and Fe/Mg values (Fig. 3). Thus, olivine xenocrysts were incorporated into angrite groundmass magma after experiencing variable degrees of oxidation. The presence of Fe-Ni metals in xenocrysts reflects early reducing conditions before oxidation. This is consistent with the fact that they are found in the most magnesian xenocrysts. It is still unclear why Cr and Ca in olivine xenocrysts are not related to Fe-Mg-Mn compositions [7].

References: [1] Yamaguchi A. et al. (2016) *Meteorite Newslett. 25*. [2] Imae N. et al. (2015) *Antarct. Record, 59*, 38-72. [3] Mikouchi T. et al. (2016) *6th Symp. Polar Sci*., NIPR, abstract. [4] McKibbin S. et al. (2016) *6th Symp. Polar Sci*., NIPR, abstract. [5] Mikouchi T. et al. (1996) *Proc. NIPR Symp. on Antarct. Meteorites*, *9*, 174-188. [6] Mikouchi T. (2014) *Antarct. Meteorites*, *XXXVII*, 49-50, NIPR, Tokyo. [7] Mikouchi T. et al. (2015) *LPS XLVI*, Abstract #2065. [8] Goodrich C. A. and Delaney J. S. (2000) *GCA*, *64*, 149-160. [9] Jambon A. (2008) *Meteoritics & Planet. Sci., 43*, 1783-1795.